

Chapter 25

Bone Mechanical Stimulation with Piezoelectric Materials

J. Reis, C. Frias, F. Silva, J. Potes, J. A. Simxes, M. L. Botelho, C. C. Castro, and A. T. Marques

INTRODUCTION

Fukada and Yasuda were the first to describe bone piezoelectrical properties, in the 1950s. When submitting dry bone samples to compressive load, an electrical potential was generated, an occurrence explained by the direct piezoelectric effect (Fukada and Yasuda, 1957). The nature of the piezoelectric effect is closely related to the occurrence of electric dipole moments in solids. In connective tissues such as bone, skin, tendon and dentine, the dipole moments are probably related to the collagen fibers, composed by aligned strongly polar protein molecules (ElMessiery, 1981; Fukada and Yasuda, 1964; Halperin et al., 2004). The architecture of bone itself, with its aligned concentric lamellae, concurs for the existence of potentials along bone structure (El-Messiery, 1981).

Bone piezoelectric constants, that is the polarization generated per unit of mechanical stress, change according to moisture content, maturation state (immature bone has lower piezoelectric constants when comparing to mature bone) and architectural organization (samples from osteosarcoma areas show lower values due to the unorganized neoplastic changes) (Marino and Becker, 1974).

Early studies concentrated on dry bone and because collagen's piezoelectricity was described as nearly zero with 45% moisture content, there were doubts that wet bone could, in fact, behave as a piezoelectric material, but further studies confirmed it in fact does (Fukada and Yasuda, 1957; Marino and Becker, 1974; Reinisch and Nowick, 1975). Some of the published studies reinforce the importance of fluid flow as the main mechanism for stress generated potentials in bone, and piezoelectricity's role was, and still is, quite unknown (Pienkowski and Pollack, 1983).

More recently, bone piezoelectrical properties have rouse interest, in the context of bone physiology and electro-mechanics. It has been associated to bone remodeling mechanisms, and to streaming potential mechanisms (Ahn and Grodzinsky, 2009; Ramtani, 2008). Piezoelectricity explains why, when under compression, collagen reorganizes its dipole and shows negative charges on the surface, which attract cations like calcium. Conversely, if tensed, collagen yields predominance of positive charges, thus obviously influencing the streaming potential and mineralization process (Noris-Suárez et al., 2007).

The commercially available biomaterials for bone replacement and reinforcement do not take into account the bone natural piezoelectricity and the mechanism of

streaming potential, and thus its use is accompanied by a break in bone natural electro physiologic mechanisms.

On the other hand, so far orthopedic implants only perform fulfill primary functions such as mechanical support, eliminating pain and re-establishing mobility and/or tribologic/articular contact. Arthroplasty is liable to cause intense changes on strain levels and distribution in the bone surrounding the implant, namely stress shielding. Metal stiffness is much higher than that of bone, so the rigid stems tend to diminish the amount of stress transmitted to the surrounding bone and produce stress concentration in other areas, depending on geometry and fixation technique. Stress shielding leads to bone resorption, which in turn may cause implant instability and femoral fracture, and make revision surgery more challenging (Beaulé et al., 2004; Huiskes et al., 1992; Mintzer et al., 1990; Sumner and Galante, 1992). Ideally, the bone implant should present sensing capability and the ability to stimulate bone, maintaining physiological levels of strain at the implant interface.

The work here summarized explores *in vitro* and *in vivo* use of a piezoelectric polymer for bone mechanical stimulation.

Piezoelectric Materials for Mechanical Stimulation of Bone Cells—The *in vitro* Study

Osteocytes and osteoblasts are essential for mechanosensing and mechanotransduction, and cell response depends on strain and loading frequency (Kadow-Romacker et al., 2009; Mosley et al., 1997). We explored the use of piezoelectric materials as a mean of directly straining bone cells by converse piezoelectric effect.

The MCT3T3-E1 cells were cultured under standard conditions and on the surface of Polyvinylidene Fluoride (PVDF) films, subjected to static and dynamic conditions, as described by Frias et al. (2010).

Polymeric piezoelectric films (PVDF) were used as substrate for cell growth. These thin films consisted of a 12 x 13 mm active area, printed with silver ink electrodes on both surfaces in a 15 x 40 mm die-cut piezoelectric polymer substrate, polarized along the thickness. In dynamic conditions the substrates were deformed by applying a 5 V current, at 1 Hz and 3 Hz for 15 min.

To guarantee adhesion of osteoblasts to the device surface and electric insulation, the surface was uniformly covered with an electric insulator material. The chosen material for covering was an acrylic, poly (methyl methacrylate) (PMMA), (PERFEX®, International Dental Products, USA), used alone in the first three layers and a in forth layer along with 4% of Bonelike® (250–500 µm) particles added (kindly offered by INESC Porto). The coating was performed by dip-coating at constant velocity of 0, 238 mm/sec. Impedance was measured both in saline and culture medium, in non-coated and coated devices, and electric insulation achieved. The coating procedure aimed improvement of cell adhesion and electrical insulation. Electrically charged particles are known to improve osteoblast proliferation and it was important to prevent cell damage and other means of stimulation other than the mechanical (Dekhtyar et al., 2008; Kumar et al., 2010; Nakamura, 2009).

To estimate the magnitude of stress/strain, finite numerical models were applied and theoretical data was complemented by optic experimental data. The finite numerical method estimated displacement varying from 6.44 to 77.32 nm in uncoated films, with strain levels around 2.2 μ strains along the surface. The Electronic Speckle Pattern Interferometry (ESPI) method showed the displacement in coated films was lower, and the maximum substrate displacement was 0.6 μ m, in the central area of the coated devices; displacement was minimum in the encastre (clamped) region.

Piezoelectric substrates (standing on culture dishes, TPP) and controls (standard culture dishes, TPP) were seeded with 16×10^4 cells, with a total volume of 100 μ l of cell suspension. Cells were allowed to adhere to the substrate, then the rest of culture medium added ($n = 6$); and cells grown in both static and dynamic piezoelectric substrates. The MCT3T3-E1 cells were cultured in standard conditions, using α -MEM medium (Cambrex), 2 mM L-Glutamine (Cambrex), 10% of bovine fetal serum (Gibco), 0.5% gentamicin and 1% amphotericin B (Gibco).

The statistical analysis was done using software Origin Pro 8 (OriginLab Corporation, USA).

Normal distribution of the results was verified using the Kolmogorov–Smirnov test, homogeneity of variance assessed through the Levene test and differences between groups tested using one-way ANOVA (at a level of 0.05).

Cell viability and metabolic activity was accessed through the resazurin method, after stimulation of dynamic group; viable cells reduce resazurin, producing resorufin, a highly fluorescent product. Previous studies indicated PVDF affects negatively adherent cell lines' viability (Hung et al., 2006; Tabary et al., 2007).

The assessment of cell viability and proliferation evidenced a material's poorer performance than control standard culture vessels, in spite of the coating procedure (Table 1). The results are expressed as percentage of the value of controls (considered as 100%) \pm standard error of the mean and show higher viability values on mechanically stimulated substrates, although the differences are not statistically significant.

Table 1. Cell viability 24 hr and 48 hr after seeding and daily stimulation of the dynamic group, results are expressed in percent related to controls (standard cell culture dish), assumed as 100%. Means and Error bars show Means \pm Standard Error of the Mean.

Proliferation and Viability	Static	Dynamic
24 hours post-seeding	49.9 \pm 5.25	59.7 \pm 15.7
48 hours post-seeding	76.4 \pm 16.9	83.4 \pm 25.1

Nitric oxide (NO) is a messenger molecule produced in response to mechanical stimulation of osteoblasts and osteocytes, with a large variety of biological functions (Smalt et al., 1997; Van't Hof, 2001). In this study, culture medium samples were collected immediately after stimulation and NO measured, using NO Assay Kit (Biochain), based on the Griess reaction, after sample deproteinization, and according to the manufacturer's instructions (Figure 1). Culture medium NO measurements in the samples subjected to mechanical stimulation were of 3.7 ± 0.65 and 3.2 ± 0.54 μ mol/ml,

respectively at 24 and 48 hr post-seeding. The nitric oxide values in static conditions were significantly lower, $2 \pm 0.35 \mu\text{mol/ml}$, 24 hr post-seeding and $1.7 \pm 0.3 \mu\text{mol/ml}$, 48 hr post-seeding (Figure 1).

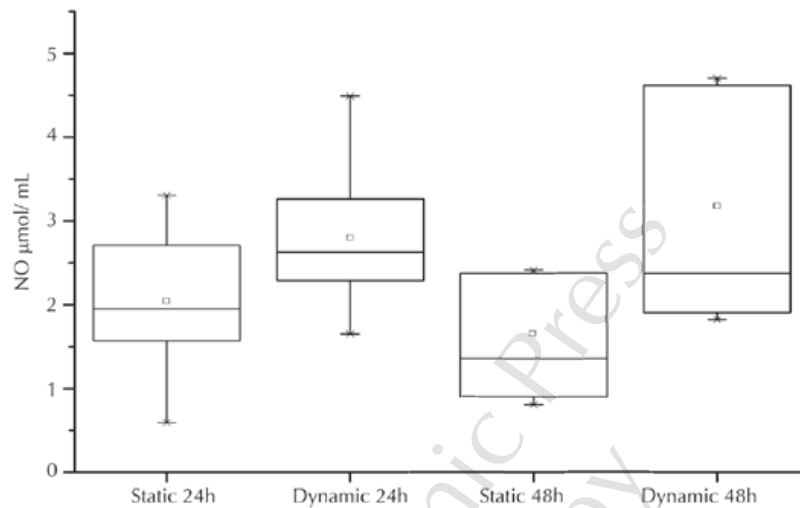


Figure 1. Nitric oxide measurement ($\mu\text{mol/ml}$) in culture medium in static versus dynamic conditions, 24 and 48 hr after seeding MC3T3 on the devices, and immediately after stimulation at 1 and 3 Hz. NO values are significantly higher in the dynamic group.

The NO measurement results of culture under dynamic conditions versus static conditions, suggest osteoblasts detect and respond in a reproducible way to small displacements and strain levels.

Changes induced by mechanical stimulation on the cytoskeleton were qualitatively assessed through indirect immunofluorescence. Primary antibodies against actin, laminin and tubulin were used; stains show stronger fluorescence on mechanically stimulated cells, clearer images of the cytoskeleton elements and nucleus delimitation and prominent cytoplasmic extensions (Figures 2 to 4).

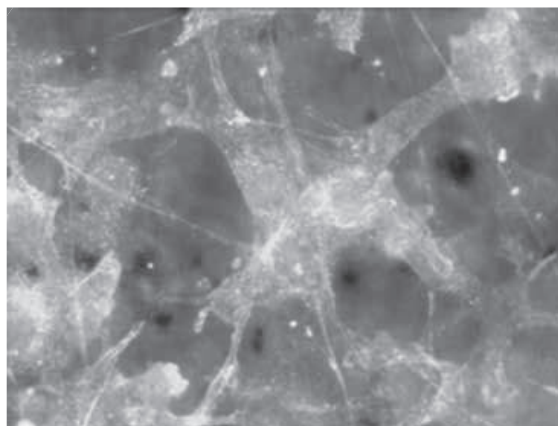


Figure 2. MC3T3 cells on the active area of the device immediately after mechanical stimulation. Indirect immunofluorescence using primary antibody against actin (Actin, pan Ab-5, Thermo Scientific, used at 1:50) and secondary antibody (Chromeo™ 488 conjugated Goat anti-Mouse IgG, Active Motif 1:500); (400X, microscope Olympus BX41, Olympus Cell A Imaging Software).

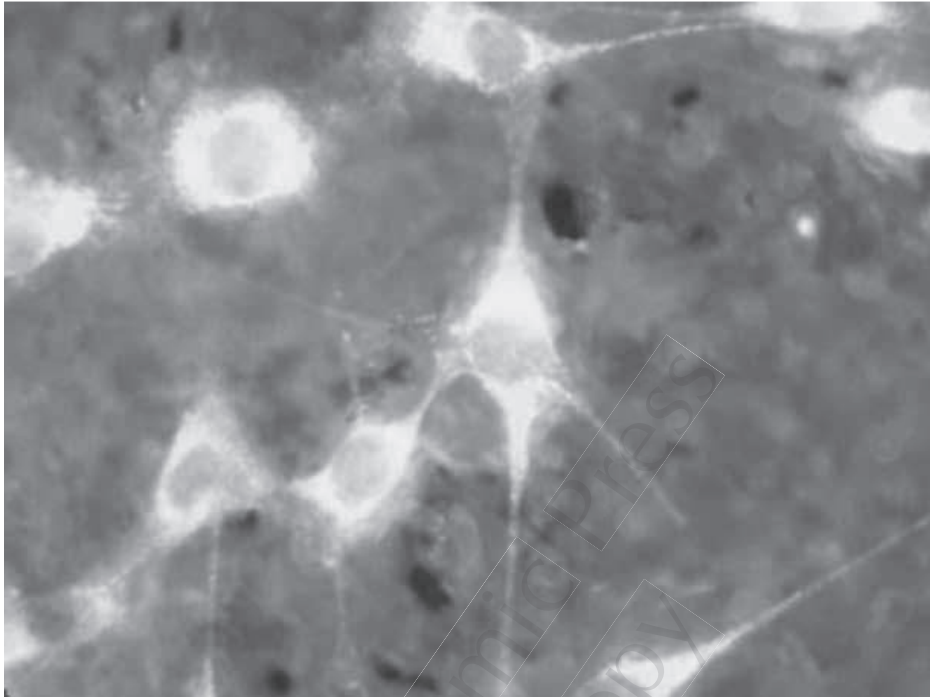


Figure 3. MC3T3 cells on the active area of the device immediately after mechanical stimulation. Indirect immunofluorescence using primary antibody against actin (Laminin, Ab-1, Thermo Scientific, used at 1:50) and secondary antibody (Chromeo™ 488 conjugated Goat anti-Rabbit IgG, Active Motif 1:500); (400X, microscope Olympus BX41, Olympus Cell A Imaging Software).

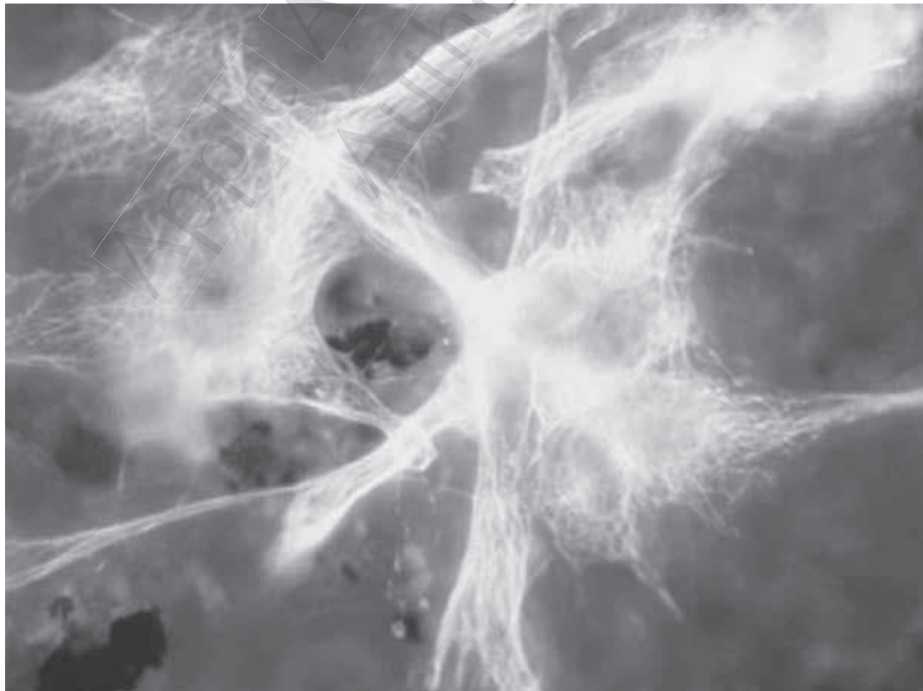


Figure 4. MC3T3 cells on the active area of the device immediately after mechanical stimulation. Indirect immunofluorescence using primary antibody against actin (Tubulin β, Thermo Scientific, used at 1:50) and secondary antibody (Chromeo™ 488 conjugated Goat anti-Rabbit IgG, Active Motif 1:500); (400X, microscope Olympus BX41, Olympus Cell A Imaging Software).

The *in vitro* study showed evidence of effective bone cell mechanical stimulation, and the concept was further explored *in vivo*. The *in vivo* implantation of piezoelectric actuators for tissue mechanical stimulation is innovative and a potential use in the development of smart implants.

Piezoelectric Materials for Bone Mechanical Stimulation—the *in vivo* Study

The actuator device was developed, composed of a micro-board containing a ultra-low power 16-bit microcontroller (eZ430-RF2500, Texas Instruments, USA), powered by lithium battery and encapsulated in polymethylmetacrilate (PMMA) and a set of six actuators composed of PVDF and silver electrodes, electrically insulated by dip-coating as previously described. A similar, but static, control device was also developed, sterilized and implanted.

The sterilization of the device posed a challenge in itself. The devices included a 16-bit processor, which corrupted its memory when submitted, in a Co-60 source, to 25 kGy at a dose rate of 2 kGy/hr. On the other hand, it was not possible to sterilize by moist or dry heat since the PVDF actuators depolarize at temperatures equal or above 60°C. An alternative sterilization method, which ensured absence of toxic residues, was developed. The methodology of its development and validation was based on ISO 11737-1 and ISO 14937, as described elsewhere (Reis et al., 2010).

The actuator device was implanted in the left hind limb and the control static device was implanted in the right hind limb of a 4 year old merino ewe, with 45 kg body-weight, under general inhalatory anaesthesia. Two osteotomies were made on the medial surface of the tibial proximal physis using an especially metal designed guide to make two regular and well orientated osteotomies using an oscillating saw. The bone was continuously irrigated with a sterile saline solution during the process of low speed drilling and cutting. The same procedure was followed with a different design guide for the distal femoral physis, where four osteotomies were done. The portion of the devices containing the microprocessor and the power supply were left in the subcutaneous space.

One week after implantation calcein (Sigma, USA) was injected subcutaneously (15 mg/kg) and 1 week prior to sacrifice the same procedure was done with alizarin complex one (25 mg/kg) (Sigma). Thirty days after implantation the ewe was sacrificed by intravenous sodium pentobarbital injection. The present study was authorized by competent national authorities and conducted accordingly to FELASA's guidelines for animal care. Proper analgesia procedures began before the surgery and were maintained through a week.

Both hind limbs were dissected, the implanted materials and surrounding tissue removed and fixed in 4% paraformaldehyde for 2 weeks. Bone samples were cut transversally to the long axis of the bone, each including a piezoelectric film and the surrounding bone

Specimens were dehydrated through an ascending ethanol series. Soft tissues (local lymph nodes and samples of the fibrous capsule surrounding the implants) were routinely processed and embedded in paraffin. Undecalcified bone samples of each of the implants were included in resin (Technovit® 9100, Heraeus Kulzer, Germany)

according to the manufacturer's instructions and 80 μm thick sections cut with a saw microtome (Leica 1600, Germany) parallel to the piezoelectric film long axis. A minimum of five sections of each resin block was cut. Sections were then appropriately processed for routine staining (Giemsa Eosin), mounted for fluorescence microscopy.

The prepared slides were evaluated qualitatively. For histomorphometric studies the interface between the bone and implant was divided in four distinct areas: A1, A2, A3, and A4, from cortical towards bone surrounding the free extremity of the piezoelectric film (Figure 5).

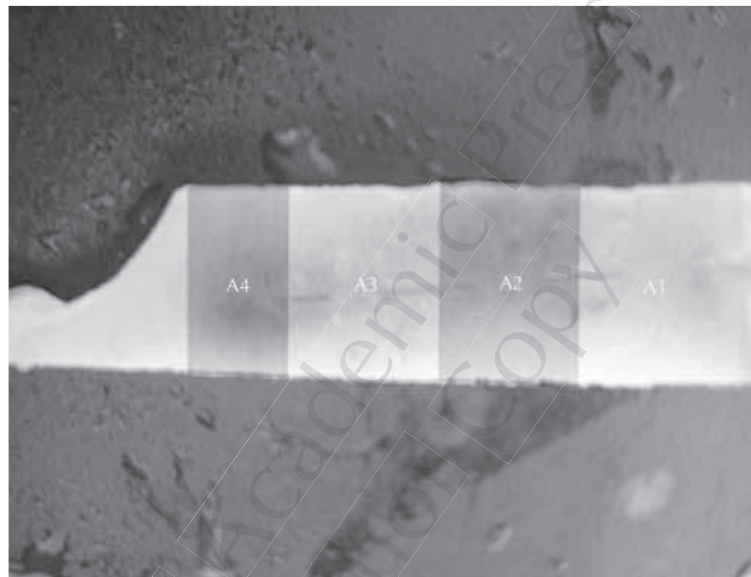


Figure 5. Tibia section the osteotomy where the piezoelectric film was placed. The figure shows example of bone section prior to inclusion and how the areas for histomorphometry were distributed; A1 corresponds to the film encastre (clamped) region.

Pictures were taken from the bone surrounding both sides of the film in areas A1 to A3 and A4.

For immunohistochemistry, bone sections were decalcified in formic acid 5% for 3 weeks, dehydrated in ethanol, cleared in xylene and embedded in paraffin wax and 3 μm sections cut. After deparaffinization and rehydration, immunohistochemistry sections were treated with 3% hydrogen peroxide for 10 min.

Primary antibodies for Proliferating Cell Nuclear Antigen (PCNA) (NeoMarkers, USA, Mouse Monoclonal Antibody, Ab-1, Clone PC10, Cat. #MS-106-P0), Osteopontin (NeoMarkers, Rabbit Polyclonal Antibody, Cat. #RB-9097) and Osteocalcin (Abcam, Mouse monoclonal [OC4-30], Cat. ab13418) were diluted to 1:200, 1:50, and 1:40, respectively. Prior to immunostaining the sections were pretreated for antigen retrieval at 100°C in 10 mM citrate buffer, pH 6, for 20 min in microwave oven, followed by cooling for 30 min at room temperature. For double staining of PCNA and osteopontin, immunohistochemistry was done using a double staining kit PicTure™ (Zymed Laboratories Inc, USA.), according with the manufacturer's instructions. Slides were counterstained with Mayer's hematoxylin and Clearmount used to mount the slides.

Osteocalcin immunohistochemistry was performed with resource to kit Picture™-MAX Polymer (Invitrogen, USA.). Slides were counterstained with Mayer's hematoxylin, dehydrated, mounted with Entellan® (Merck, Germany), and covers lipped. For all sections positive controls were made simultaneously. As negatives controls adjacent sections were incubated: (a) without primary antibody and, (b) with rabbit/rat normal serum (similar concentration as that of primary).

After one month implantation period, there were statistically significant differences. Total bone area around the actuators was significantly higher, when comparing to static controls ($39.91 \pm 14.08\%$ vs $27.20 \pm 11.98\%$) (Figure 6).

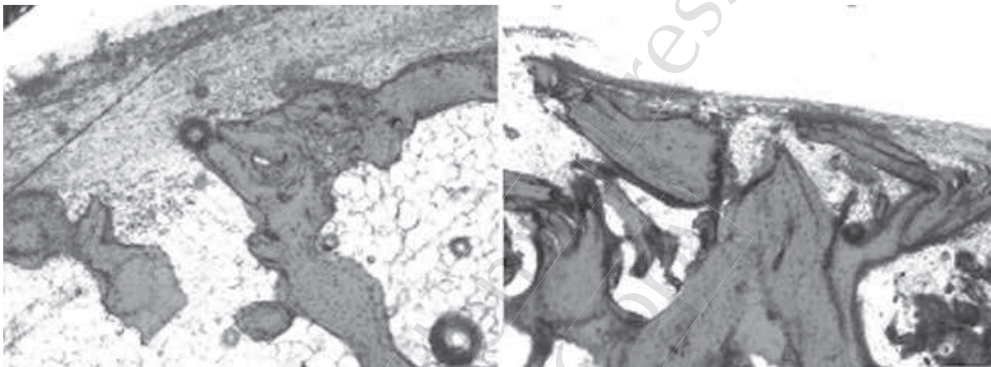


Figure 6. Microphotograph of undecalcified sections, Giemsa-Eosin stain, of A3 area of static control (on the right) and actuator (on the left). Both were implanted in the same position in the tibia. A fibrous capsule was present on the bone/film interface. Scale bar represents 200 μm .

The increment of bone occupied area was due to new bone formation, as evidenced in Figure 7. In actuators the area occupied by woven bone and osteoid was $64.89 \pm 19.32\%$ of the total bone area versus $31.72 \pm 14.54\%$ in static devices. With the aid of the fluorochrome labeling, we measured bone mineral deposition rate in the distal third of the piezoelectric devices. Bone deposition rate was significantly higher around actuated devices ($4.44 \pm 1.67 \mu\text{m}/\text{day}$) than around static devices ($2.70 \pm 0.95 \mu\text{m}/\text{day}$).

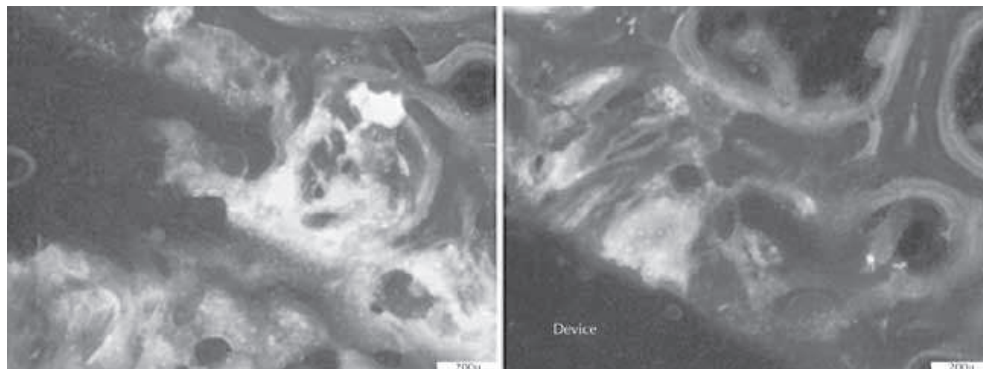


Figure 7. Microphotograph of undecalcified sections, unstained; the fluorochromes calcein (green) and alizarin complexone (red) signal the areas of newly formed bone around one of the actuators placed in the femur; picture on the left shows A4; picture on the right shows A3. Scale bar represents 200 μm .

Newly formed bone and increase in total bone area were unevenly distributed along the length of the actuators; significant differences when comparing actuators to static controls arose from the two distal thirds of the devices. No differences in total bone area and new bone area were found in the actuators encastre region (clamped region). These findings are in agreement with the previous Finite Numerical Method and ESPI method studies on the displacement of the piezoelectric films under the experimental conditions.

Immunohistochemistry shows a marked elevation in osteopontin detection around actuators, in A3 and A4 (Figure 8). Since it is known that OPN production is increased in association with mechanical loading (Harter et al., 1995; Perrien et al., 2002), the increased expression we found around actuators' areas of higher deformation, when comparing to static controls, is most likely associated with mechanical stress. No marked differences were found in PCNA detection.

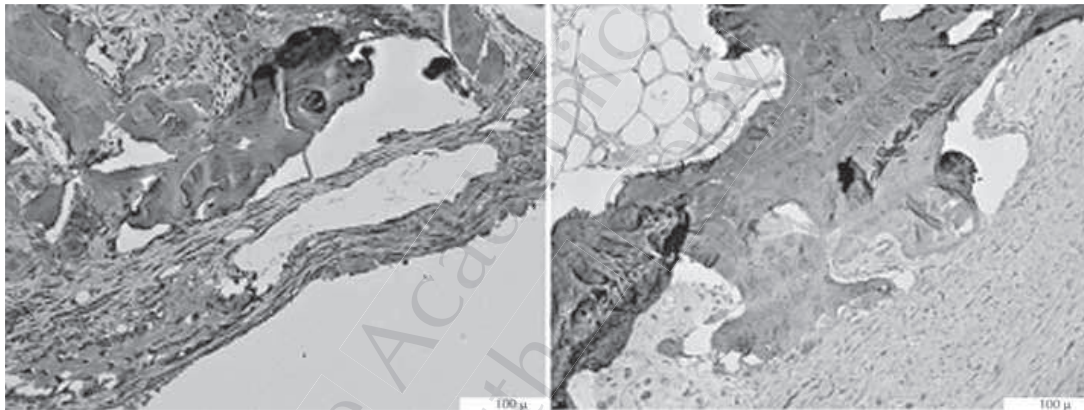


Figure 8. Microphotograph of decalcified sections, double Fast-Red and DAB immunohistochemistry staining for osteopontin and PCNA, respectively. Picture shows A3 areas of actuator (on the left) and static control (on the right), evidencing much more extensive osteopontin labelling around actuator. Scale bar represents 100 μm .

Osteocalcin detection was also increased around actuators, when compared to controls (Figure 9). Osteocalcin is a non-collagenous protein and a major constituent of bone matrix; it is produced by osteoblasts and binds strongly to hydroxyapatite; osteocalcin is considered a sensitive marker of bone formation, and it has been described as rising as consequence of mechanical stimulation-induced cell differentiation (Mikuni-Takagaki, 1999; Pavlin et al., 2001).

We observed that all the devices were separated from neighbouring bone by a fibrous capsule with an average thickness of 292 μm . This is probably due to the material itself, since the fibrous capsule was obvious both in actuators and static devices, with no statistical significant differences in capsule thickness between the two groups (289.59 \pm 131.20 μm in actuated films vs 293.93 \pm 84.79 μm). It would be mandatory to develop and test a material with improved biocompatibility to evaluate accurately the bone material interface.

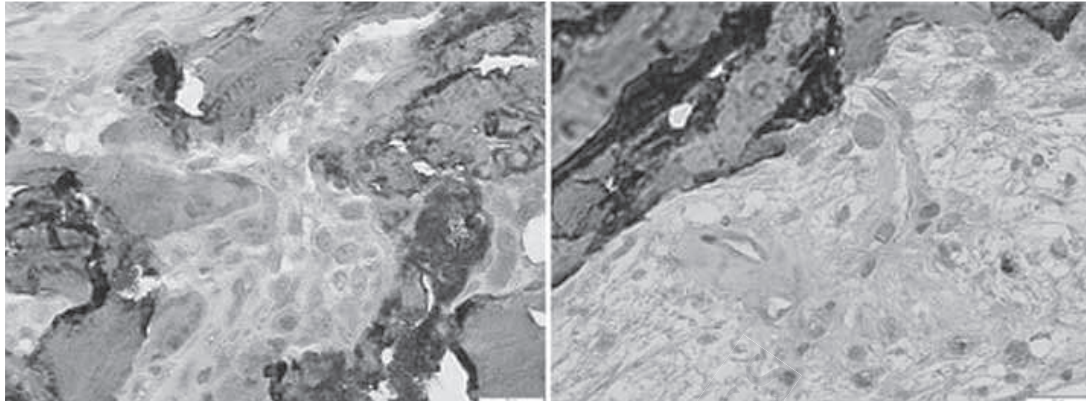


Figure 9. Microphotograph of decalcified sections, DAB immunohistochemistry staining for osteocalcin, respectively. Picture shows A3 areas of actuator (on the left) and static control (on the right), evidencing more extensive osteocalcin labelling around actuator. Scale bar represents 20 μm .

The results are very clear in evidencing qualitative and quantitative statistically significant differences when comparing static and actuated films but it would be necessary to enlarge the animal study. However, considering the limitations evidenced by the material itself, we feel this could be ethically questionable unless alternative electrodes and materials with piezoelectric properties are developed.

CONCLUSION

The huge potential of piezoelectric materials as a mean to produce direct mechanical stimulation lies also on the possibility of producing stimuli at a high range of frequencies and in multiple combinations, in order to avoid routine loading accommodation.

The use of piezoelectric material based actuators to produce bone mechanical stimulation seems promising in theory and the present *in vitro* and *in vivo* studies were a first step towards the validation of the concept.

Taking into account what is already known on bone physiology, and particularly, bone mechanotransduction, developing materials for bone regeneration that are able to respect bone electrophysiology seems like a logical move towards better clinical results whenever treatment of bone defects is being considered.

KEYWORDS

- Actuator device
- Nitric oxide
- Osteoblasts
- Osteocytes
- Piezoelectric effect
- Polymeric piezoelectric films